HTD-Vol. 171, Heat Transfer in Electronic Equipment
ASME 1991

THE EFFECT OF COMMON DESIGN PARAMETERS ON THE THERMAL PERFORMANCE OF MICROELECTRONIC EQUIPMENT: PART II – FORCED CONVECTION

J. R. Culham, S. Lee, and M. M. Yovanovich
Department of Mechanical Engineering
Microelectronics Heat Transfer Laboratory
University of Waterloo
Waterloo, Ontario, Canada

Abstract

Designers of microelectronic circuitry have very few options available to them in their efforts to control temperature related failures. Some of the design options, such as the thermal conductivity and surface emissivity of the circuit board, the flow velocity of the cooling fluid and the positioning and power dissipation of the heat sources are examined here in order to determine the relative merit of each as a means of controlling circuit board temperatures.

META - an analytical/numerical conjugate heat transfer model is used to calculate temperature distributions in a test circuit board in which the above mentioned design conditions are varied over a range of values typically found in microelectronic applications.

Nomenclature

c_p	specific heat, $J/(kg \cdot C)$
d	dimensionless distance between heat sources
h	heat transfer coefficient, $W/(m^2 \cdot K)$
k	thermal conductivity, $W/(m \cdot K)$
ℓ	heat source length and width, m
L	total circuit board length, m
Nu_2	Average Nusselt Number of second heat source, $\equiv q_{j,2} \cdot \ell/(\overline{\Delta T_2} k_f)$
Pe	Peclet number, $\equiv u_\infty \cdot L/\alpha$
Pr	Prandtl number, $\equiv \nu/\alpha$
q	heat flux density, W/m^2
Re	Reynolds Number $u_\infty \cdot L/\nu$
t	board thickness, m
T	temperature, K
u, v, w	boundary layer velocity in the x, y and z-direction, respectively, m/s
u_∞	free stream velocity, m/s
W	circuit board width, m
x, y, z	Cartesian coordinates

Greek Symbols

α	thermal diffusivity, $\equiv k_f/(\rho \cdot c_p)$, m^2/s
ϵ	emissivity
ϕ	relative temperature change in the downstream heat source, $\equiv (\Delta T_2 - \Delta T_{2,0})/\Delta T_{2,0}$
ρ	density, kg/m^3
θ	dimensionless temperature excess, $\equiv (T - T_a)/T_{ref}$
ν	kinematic viscosity, m^2/s
σ	Stefan-Boltzmann constant, $\equiv 5.67 \times 10^{-8}$, $W/(m^2 \cdot K^4)$

Subscripts

f	fluid
j	Joulean
r_1, r_2	radiation from the front and back surfaces, respectively
ref	reference
s	solid
sk	sink
w_1 w_2	front and back wall, respectively
∞	free stream

Superscripts

$*$	dimensionless variable

Introduction

The thermal design of microelectronic equipment has assumed a more prominent role in recent years due to the trend towards increased component packaging densities and higher powered integrated circuits. Circuit designers are faced with maintaining junction temperatures at or below 100 °C while trying to design circuit boards which do not compromise electrical behavior. Computer Aided Design tools, based on finite element or finite difference techniques are often used to perform the rigorous thermal assessment required throughout the many design processes required in the development of microelectronic circuit boards. However, the many tradeoff studies required during the initial stages of the design process restrict the use of most numerical based CAD tools because of the cost involved in setting up and running parametric studies.

As opposed to the detailed temperature map required during the latter stages of the design process, the circuit designer rarely requires such detail during the initial stages of circuit design. Instead, the circuit designer is more intent on establishing the upper and lower bounds of operating temperature given the preliminary design layout and the thermophysical properties of the materials proposed for the circuit design. The intent of this paper is to provide a feel for the sensitivity of the various parameters over which a designer has some control. The effect each of these parameters has on component or heat source temperature will be presented for a range of values typically observed in circuit board design.

Thermal Model

A microelectronic circuit board, as shown in Fig. 1, has a complex temperature field, established through the thermal interaction of many discrete heat sources with a multilayer circuit board and the boundary layer, which may be laminar or turbulent, depending on the nature of the forced flow. The enlarged illustration in Fig. 1 shows a side view of the circuit board/heat source interface where the pertinent methods of heat dissipation involved in the cooling process are shown.

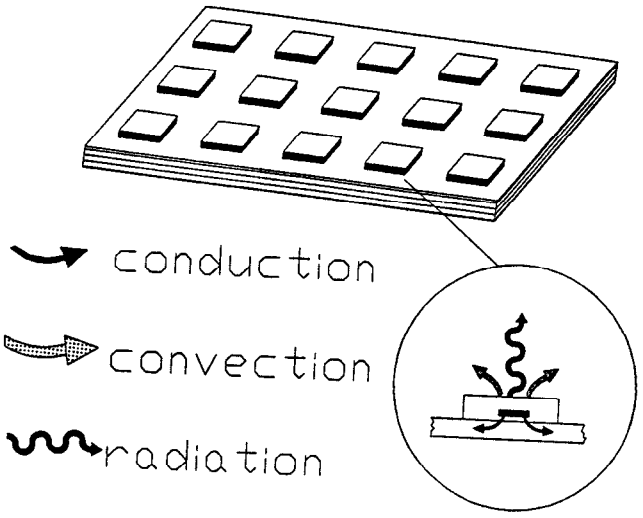

Figure 1: Conjugate Heat Transfer From a Typical Circuit Board

The complexity of the temperature field is also reflected in the governing equations describing the thermal behavior and the associated boundary conditions, as given in Eqs. (1-13). As a result an exact analytical solution is not available with present solution techniques. However, approximate methods, which significantly simplify the solution technique, can be used to obtain accurate solutions to highly complex conjugate heat transfer problems. Assumptions which simplify the analytical modeling but do not detract from the accuracy or the physical integrity of the solution are given as follows:

1. Heat sources are assumed to be flush mounted with the surface of the printed circuit board, representative of chip-on-board or surface mount technology.

2. The circuit board aspect ratio, defined as the total length of the board in the flow direction over the thickness of the board (L/t), is of the order 125:1. The predominant surfaces for convective cooling are the upper and lower surfaces of the circuit board, which encompass approximately 99% of the total exposed surface area of the board. Therefore, the heat transfer through the edges of the board is considered negligible and these surfaces will be treated as adiabatic.

3. Although the convective heat transfer coefficient varies significantly over the surface of an electronic circuit board, cooled by forced convection, typical values of the Biot Number ($\mathrm{Bi} = ht/k_s$) range from 0.0003 to 0.1. The magnitude of the Biot number serves as an indication of the relative magnitude of the thermal resistance across the thickness of the board to the thermal resistance within the fluid boundary layer. Since it is commonly accepted that a $\mathrm{Bi} < 0.1$ allows a two-dimensional conduction analysis to be used with minimal deviation from results obtained using a more rigorous three-dimensional solution, a two-dimensional assumption will be used in the iterative model.

4. The cooling fluid is taken to be dry air with flow over the circuit board assumed to be steady, two dimensional and incompressible.

5. The maximum flow velocity anticipated in microelectronic applications is low enough that viscous dissipation can be considered negligible.

6. Since the component packages are assumed to be flush mounted the pressure difference through the boundary layer can be assumed uniform.

7. the circuit board has a uniform thickness with heat dissipating component packages being in perfect contact with the surface

of the circuit board.

8. The power dissipated by the components is assumed to be steady and invariant with respect to time.

Boundary Layer Equations

Equations (1 - 3) are the conventional boundary layer equations where mass, momentum and energy are conserved within the domain of the boundary layer while the diffusion of momentum and energy in the direction parallel to the flow is considered negligible.

The velocity term across the flow direction (v) is deemed to be much smaller than the u-velocity and therefore can be dropped from the full three dimensional boundary layer equations. The two dimensional equations and their associated boundary conditions significantly simplify the boundary layer analysis without an appreciable loss of accuracy when compared with experimental results. All fluid thermophysical properties are assumed constant throughout the analysis.

$$\frac{\partial u}{\partial x} + \frac{\partial w}{\partial z} = 0 \tag{1}$$

$$u\frac{\partial u}{\partial x} + w\frac{\partial u}{\partial z} = \nu\frac{\partial^2 u}{\partial z^2} \tag{2}$$

$$u\frac{\partial T}{\partial x} + w\frac{\partial T}{\partial z} = \alpha\frac{\partial^2 T}{\partial z^2} \tag{3}$$

where the following boundary conditions are applied

$$\text{as } z \to \pm\infty \quad , \quad u \to u_\infty, \quad T = T_a \tag{4}$$

$$\text{at } x = 0 \quad , \quad u = u_\infty, \quad T = T_a \tag{5}$$

$$\text{at } z = 0 \quad , \quad u = w = 0 \tag{6}$$

As mentioned above these boundary conditions apply for all values of $0 \leq y \leq W$, where edge losses are assumed negligible.

Solid-Side Equations

The three-dimensional Laplace equation for heat flow in a homogeneous solid is

$$\frac{\partial^2 T}{\partial x^2} + \frac{\partial^2 T}{\partial y^2} + \frac{\partial^2 T}{\partial z^2} = 0 \tag{7}$$

where the boundary conditions along the edges of a flat plate, considered to be adiabatic, can be written as

$$\text{at } x = 0 \text{ and } L \qquad \frac{\partial T}{\partial x} = 0 \tag{8}$$

$$\text{at } y = 0 \text{ and } W \qquad \frac{\partial T}{\partial y} = 0 \tag{9}$$

The boundary conditions along the planar surfaces, at the front surface of the board, denoted as $z = 0$, and the back surface of the board, denoted as $z = -t$ are given as

$$\text{at } z = -t \qquad T(z = -t^+) = T(z = -t^-) \tag{10}$$

$$k_s \left.\frac{\partial T}{\partial z}\right|_{-t+} = q_{w_1} + q_{r_1} \tag{11}$$

$$\text{at } z = 0 \qquad T(z = 0^-) = T(z = 0^+) \tag{12}$$

$$k_s \left.\frac{\partial T}{\partial z}\right|_{0-} = q_j - q_{w_2} - q_{r_2} \tag{13}$$

where q_{w_1} and q_{w_2} represent convective heat flux distributions over the front and back surfaces of the board, respectively. The wall heat flux over both surfaces can be written as

$$q_{w_1} = k_f \left.\frac{\partial T}{\partial z}\right|_{-t-} \tag{14}$$

$$q_{w_2} = -k_f \left.\frac{\partial T}{\partial z}\right|_{0+} \tag{15}$$

The radiative heat flux distribution, q_{r_1} and q_{r_2}, from the front and back of the circuit board can be expressed in terms of the Boltzmann equation, as

$$q_{r_i} = \epsilon\sigma(T_{w_i}^4 - T_{sk}^4) \qquad \text{for } i = 1,\ 2 \tag{16}$$

where the emissivity is assumed constant over each surface and the sink temperature is assumed to be the same as that of the free stream fluid.

If the Biot number ($\mathrm{Bi} = ht/k_s$), which is a measure of the internal thermal resistance of the solid to the external thermal resistance within the boundary, is less than 0.1 then the temperature difference across the thickness of the solid is small and a single average value of the cross sectional temperature can be used thus reducing the dimensional dependency of the governing equation by a factor of one.

By integrating Laplace's equation across the thickness of the board the interfacial conditions are absorbed into the governing equation, and Eqs. (7), (11) and (13) reduce to a two-dimensional fin equation:

$$\frac{\partial^2 T}{\partial x^2} + \frac{\partial^2 T}{\partial y^2} + \frac{1}{k_s t}(q_j - q_r - q_w) = 0 \tag{17}$$

where $q_w = q_{w_1} + q_{w_2}$ and $q_r = q_{r_1} + q_{r_2}$.

META, a conjugate heat transfer modeling routine developed by the Microelectronics Heat Transfer Laboratory, (Culham et al., 1991) combines an analytical boundary layer solution with a finite volume solid body solution, as described in the preceding discussion. The boundary layer solution is based on existing solution methods (Kays, 1966) for laminar boundary layer flows over flat plates where the integral form of the boundary layer equations are solved, given a flux

specified boundary condition. The resulting formulation for the local Nusselt number is used as the surface convective condition in the solid body model, as presented by Culham and Yovanovich, 1987. The two solutions are coupled using an iterative procedure to give a unique temperature profile at the fluid-solid interface which simultaneously satisfies the governing equations in both the fluid and the solid domains.

META is a diverse model, which has the capabilities of modeling conjugate heat transfer with either natural, forced or mixed convection, channel flow, laminar or turbulent flows and conduction within chip carriers for the purpose of calculating junction temperatures. In order to clearly accentuate the behavior of certain design parameters, some modeling options, such as package resistances and channel flow conditions, have been relaxed to a simpler form i.e., thin film sources and free stream flow conditions.

Parametric Analysis

The basic parameters used in the governing equations and the boundary conditions can be expressed in a dimensionless form as follows:

$$x^* = x/L \quad (18) \qquad z^* = z/L \quad (19)$$
$$u^* = u/u_\infty \quad (20) \qquad w^* = w/u_\infty \quad (21)$$
$$t^* = t/L \quad (22) \qquad \theta = (T - T_\infty)/\Delta T_{ref} \quad (23)$$

where

$$\Delta T_{ref} = \overline{q_j}\, L/k_f \quad (24)$$

where the average heat flux over the front and back surface of the board is defined as

$$\overline{q_j} = \frac{\sum Q_i}{2 \cdot (L \cdot W)} \quad (25)$$

Non-dimensionalizing the governing equations

$$\frac{\partial u^*}{\partial x^*} + \frac{\partial w^*}{\partial z^*} = 0 \quad (26)$$

$$u^* \frac{\partial u^*}{\partial x^*} + w^* \frac{\partial u^*}{\partial z^*} = \frac{1}{\mathrm{Re}} \frac{\partial^2 u^*}{\partial (z^*)^2} \quad (27)$$

$$u^* \frac{\partial \theta}{\partial x^*} + w^* \frac{\partial \theta}{\partial z^*} = \frac{1}{\mathrm{Pe}} \frac{\partial^2 \theta}{\partial (z^*)^2} \quad (28)$$

where the following boundary conditions apply.

$$\text{as } z^* \to \pm\infty \ , \ u^* \to 1, \theta = 0 \quad (29)$$

$$\text{at } x^* = 0 \ , \ u^* = 1, \theta = 0 \quad (30)$$

$$\text{at } z^* = -t^* \text{ and } 0 \ , \ u^* = w^* = 0 \quad (31)$$

where

$$\mathrm{Re} = \frac{u_\infty \cdot L}{\nu} \quad (32)$$

$$\mathrm{Pe} = \frac{u_\infty \cdot L}{\alpha} = \mathrm{RePr} \quad (33)$$

The two-dimensional solid body equations can be expressed as

$$\frac{\partial^2 \theta}{\partial (x^*)^2} + \frac{\partial^2 \theta}{\partial (y^*)^2} + \frac{k_f L}{k_s t} \left[q_j^* - q_r^* - q_w^* \right] = 0 \quad (34)$$

where

$$\text{at } x^* = 0 \text{ and } 1 \quad \frac{\partial \theta}{\partial x^*} = 0 \quad (35)$$

$$\text{at } y^* = 0 \text{ and } \frac{W}{L} \quad \frac{\partial \theta}{\partial y^*} = 0 \quad (36)$$

and the q^*'s in Eq. (34) are defined as

$$q^* = \frac{q}{\overline{q_j}} \quad (37)$$

where the subscripts j, r and w refer to the Joulean, radiative and wall components.

The solution to the governing equations for conjugate heat transfer, given in Eqs. (26 - 28) and Eq. (34), can be expressed in terms of the following eight parameters.

$$\boxed{\theta_w = \theta_w(x^*, y^*, \mathrm{Re}, \mathrm{Pe}, \frac{W}{L}, \frac{k_f L}{k_s t}, q_j^*, q_r^*)} \quad (38)$$

This is an implicit non-linear equation because of the fourth order dependency of the radiation term, q_r^*, on θ_w. The implicit nature of the wall temperature equation necessitates the use of an iterative solution technique in META, the computational model used in this analysis.

When the Biot number is greater than 0.1, and temperature gradient across the thickness of the board is not negligible, then the fourth term in Eq. (38), $k_s t/k_f L$, must be treated as two separate terms, namely k_s/k_f and t/L.

Default Conditions

Because of the inherent complexity of microelectronic circuit boards and the arrangement of IC packages, an endless combination of configurations could be selected for this study. Instead, a conventional two heat source circuit board, as shown in Fig. 2, will be analysed, where dimensions, flow conditions and thermophysical properties for the default case are given as

Board : $L \times W \times t = 0.2\ (m) \times 0.1\ (m) \times 0.0016\ (m)$
$k_s = 2\ (W/(m \cdot K))$
$\epsilon = 0$

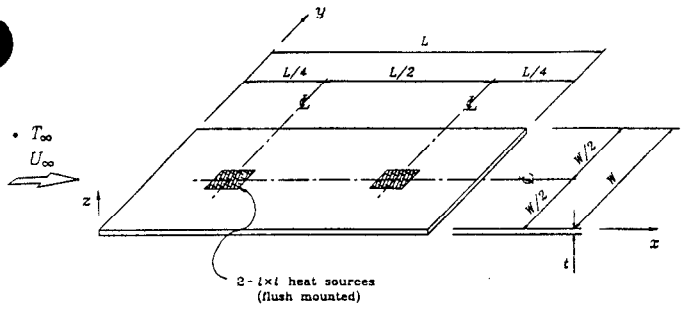

Figure 2: Geometry and Configuration of Printed Circuit Board

Heat Sources : $\ell \times \ell = 0.02\ (m) \times 0.02\ (m)$
$\epsilon = 0$
$Q_1 = Q_2 = 2\ (W)$

Fluid : $k_f = 0.0263\ (W/(m \cdot K))$
(air @ 300 K) $\nu = 15.89 \times 10^{-6}\ (m^2/s)$
$\mathrm{Pr} = 0.707$
$u_\infty = 5\ (m/s)$
$T_\infty = 293\ (K)$

Discussion

Figure 3 shows the heat flux, temperature and heat transfer coefficient distribution for the default case where $k_s = 2\ W/(m \cdot K)$, $\epsilon = 0$, $u_\infty = 5\ m/s$ and $Q_1 = Q_2 = 2\ W$. Air flow for each figure is in the positive x direction.

Figure 3.a shows a three-dimensional view of the heat flux distribution for the default conditions. Typical of most forced convection applications, the developing boundary layer near the leading edge of the circuit board provides a lower thermal resistance to heat flow across the boundary layer than corresponding downstream locations. Hence, the peak heat flux over the first source is slightly larger than that of the second source for a similar level of Joulean heating. This creates a situation in conjugate heat transfer applications where the heat conduction within the board is primarily in the negative x-direction, counter to the primary heat flow within the boundary layer.

The heat flux near the downstream edges of the packages is higher than in the centerline wake of the package. Again, this can be more clearly understood by examining the plot of heat transfer coefficient in Fig. 3.c. Downstream of the heat sources the heat transfer coefficient approaches zero as the boundary layer grows rapidly. The edges of the heat sources, parallel to the flow direction offer an alternate heat flow path of lower resistance, as shown in Fig. 3.c. Therefore the heat tends to flow within the circuit board perpendicular to the flow direction, showing the most pronounced increase immediately

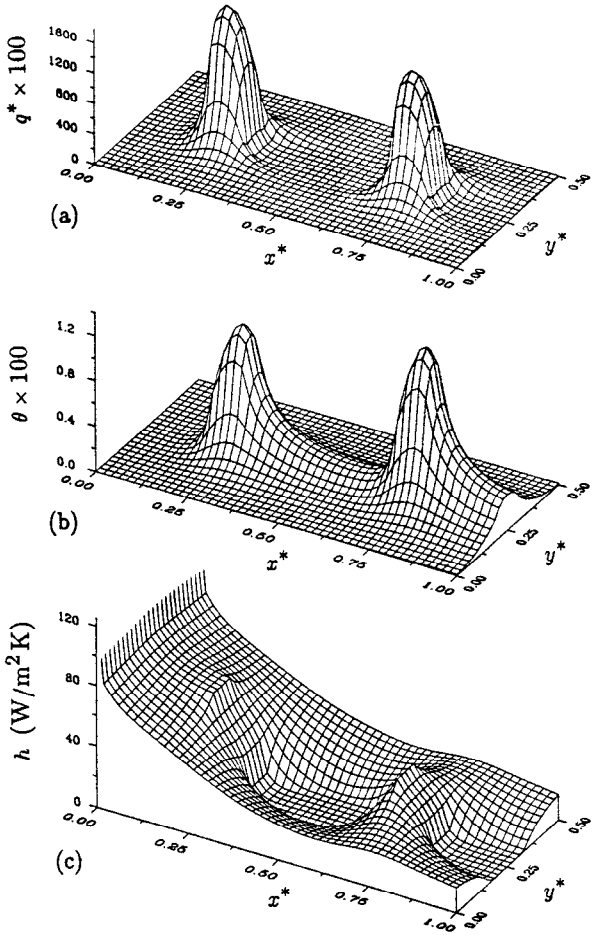

Figure 3: Dimensionless Heat Flux, Temperature and Heat Transfer Coefficient Distributions for the Default Conditions

downstream of the heat sources.

Figure 3.b shows the dimensionless temperature, defined as

$$\theta = \frac{T - T_\infty}{q_j L / k_f} \tag{39}$$

For sources of equal power dissipation cooled by forced convection, the temperature of the downstream source will always be greater than the upstream source, for constant free stream conditions, due to heat propagation within the wake.

Although the heat transfer coefficient distribution is shown over the full range of x and y in Fig. 3.c, it is not defined at $x = 0$ and at $y = 0$ or $y = W$. The heat transfer coefficient is a useful tool for estimating the local convective potential, but it should be remembered that the heat transfer coefficient is a derived quantity and is not meaningful over the full domain of x and y.

The default case, described above, will be used as the reference for other examples where the thermal conductivity and the emissivity of the printed circuit board, the flow velocity of the cooling fluid (air) and the applied power to the heat sources are varied over a range typically observed in microelectronics applications.

Figures 4 - 7 show the effect the control parameters have on dimensionless temperature. Temperature profiles are taken along the centerline of the packages in the positive x direction. In each instance a single parameter is varied, and the other default parameters are maintained.

Thermal Conductivity

The thermal conductivity of the circuit board plays a major role in the distribution of heat. Typically, a circuit board consists of alternating layers of highly conductive tracking material, usually copper, separated by a low conductivity, insulating material such as fiberglass-epoxy. Thermal modeling of laminated materials can be accomplished in one of two ways. A more exact, but more complicated method is to treat each layer individually as a homogeneous substance. The temperature fields of the individual layers are coupled through appropriate boundary conditions at the interfaces, allowing a temperature profile of the full cross section to be obtained. Secondly, a more practical method of determining the temperature profile of a laminated material is to calculate an effective thermal conductivity, based on the harmonic mean (Lemczyk et al., 1991) of the component thermal conductivities calculated using the series and parallel resistive paths with the laminates. The following discussion of thermal conductivity assumes a single homogeneous value for the entire circuit board.

The effect of board thermal conductivity on dimensionless temperature is shown in Fig. 4, where the dotted line represents the temperature profile for the default conditions. The peak temperature over each source is strongly influenced by a change in the thermal conductivity of the board. As the thermal conductivity becomes large the heat flows unrestricted within the solid and an isothermal condition is attained. Increasing the thermal conductivity is an effective means of reducing localized temperature spikes, however, an increase in thermal conductivity is principally obtained by increas-

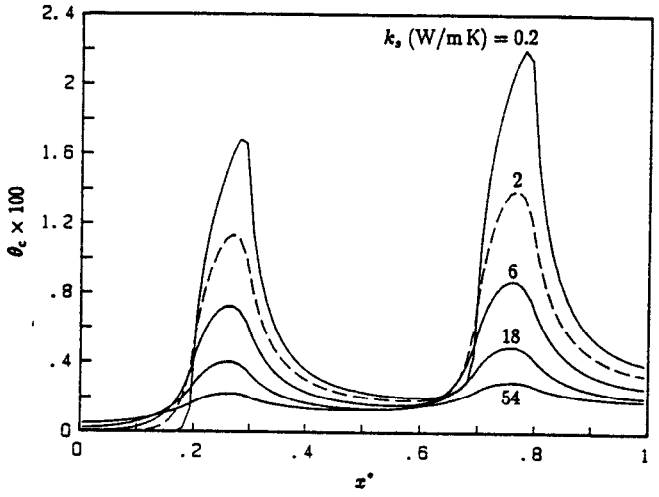

Figure 4: Centerline Temperature Profile for a Range of Circuit Board Thermal Conductivities Between 0.2 and 54 $W/m \cdot K$

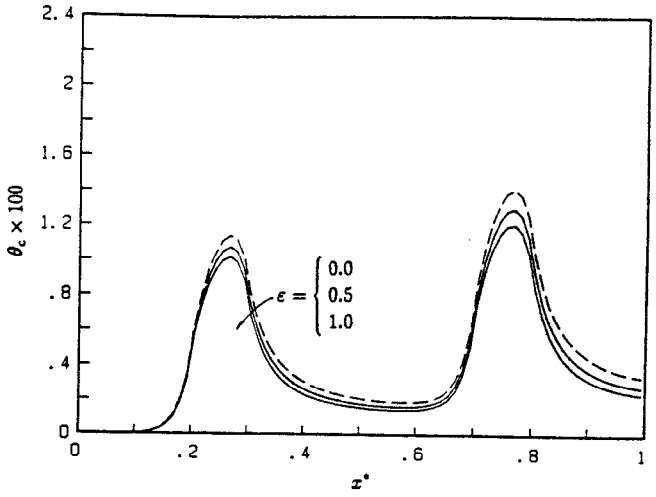

Figure 5: Centerline Temperature Profile for a Range of Circuit Board Emissivities Between 0.0 and 1.0

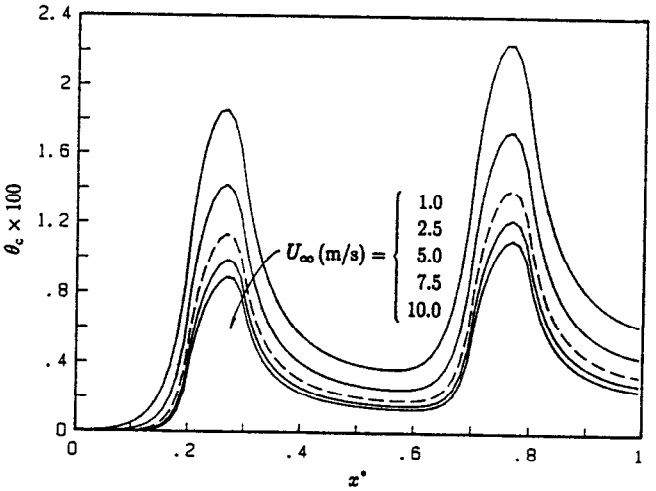

Figure 6: Centerline Temperature Profile for a Range of Circuit Board Flow Velocities Between 1.0 and 10.0 m/s

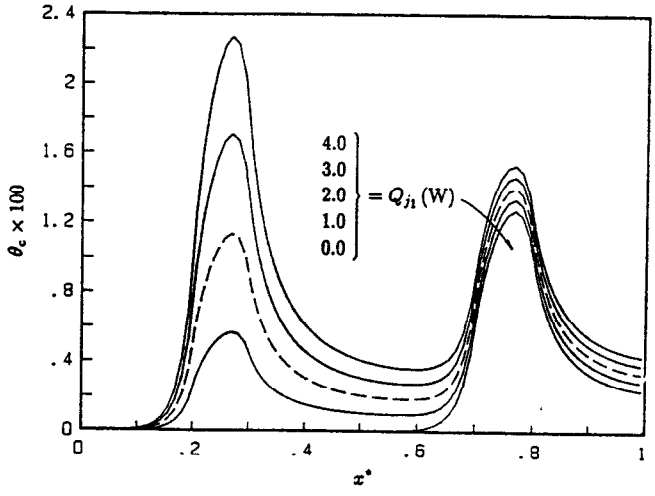

Figure 7: Centerline Temperature Profile for Changes in the Joulean Heat Dissipation of the Upstream Source

ing the copper content of the circuit board, resulting in a significant increase in cost.

Surface Emissivity

In forced convection, the effect of radiative heat transfer is significantly smaller than in a similar circuit board cooled only by natural convection (Lee et al., 1991). However, radiation can account for as much as 10% of the total heat dissipation in microelectronic applications using forced air flow. Figure 5 shows the effect a change in surface emissivity has on the dimensionless temperature of the printed circuit board. Applications in which the sink temperature is close to room temperature (293 K) a radiative heat transfer coefficient can be calculated which is approximately 5-6 $W/m^2 \cdot K$ over the full working range of temperature in a circuit board ($\approx$ 293K - 393K). This compares with the convective heat transfer coefficient, shown in Fig. 3.c, which for the default case ranges between infinity at the leading edge of the board (nominally 80-100 $W/m^2 \cdot K$) to a negligible value downstream of the heat sources.

Air Flow Velocity

The board temperature is affected by the free stream velocity through the square root of the Reynolds number in forced convection. As shown in Fig. 6, the rate at which the board temperature is lowered for increasing velocity is diminished as the free stream velocity increases. In addition to the diminishing returns attained for higher velocities, a practical limit of flow velocity of between 5 and 10 m/s is mandated for most office environments due to noise constraints. Where noise constraints are not applicable, flow velocity can be an effective means of controlling board temperatures.

Source Strength

Figure 7 is a plot of the centerline temperature profile for changes in the strength of the upstream heat source (source 1). The addition of Joulean heating has the expected effect of linearly increasing the peak temperature of heat source 1 but the peak temperature of the second heat source is also increased due to both conduction through the board and advection within the boundary layer. With a board conductivity of 2 $W/m \cdot K$, local Joulean heating accounts for approximately 90% of the temperature rise over the second source while heating of the second source because of its location in the wake of the first source accounts for 10% of the peak temperature of the second source.

Source Location

Figure 8 shows how the dimensionless temperature of the second source changes when the first source is moved from the leading edge to the trailing edge of the board.

When $\tilde{d}$, the distance between the center line of the two heat sources divided by the source length (ℓ) is equal to zero, the two sources overlap, and the temperature distribution is identical to a single source with twice the heat dissipation. Since the forced convection problem is linear, the resultant temperature is twice that of $\Delta T_{2,0}$.

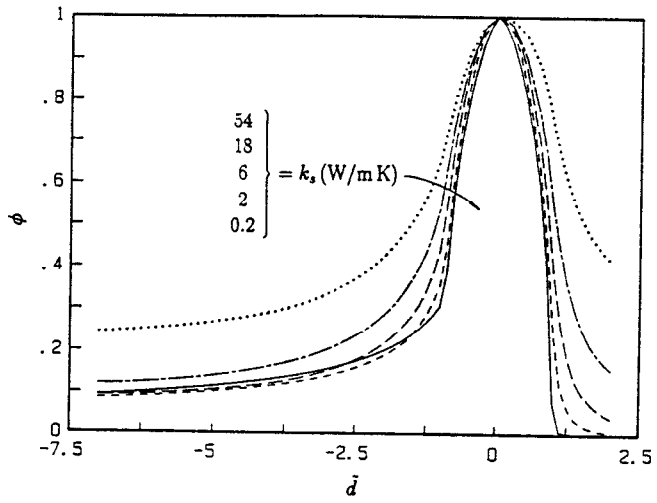

Figure 8: The Effect of the Upstream Heat Source Location on the Peak Temperature of the Downstream Heat Source

$$\phi = \frac{\Delta T_2 - \Delta T_{2,0}}{\Delta T_{2,0}} \tag{40}$$

where $\Delta T_{2,0}$ is the average temperature excess of the second source when the second source is the only source on the board.

Parameter Summary

Figure 9 is a summary of the effects that each of the controlled parameters has on the average Nusselt number over the second or downstream heat source. The ordinate scale for thermal conductivity is on the right side of the graph while the ordinate for all other parameters is on the left hand axis.

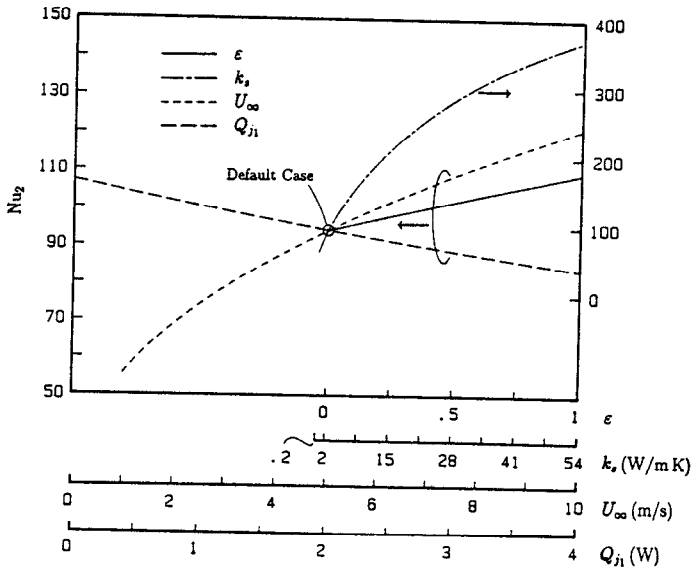

Figure 9: The Effect of Changes in the Selected Design Parameters on the Average Nusselt Number of the Downstream Heat Source

The thermal conductivity is the most effective parameter for increasing the Nusselt number over the second source and in turn decreasing the temperature. The multiple scales on the abscissa are arranged such that the node in the center of the curves is the default case. The resultant Nusselt number, which is indicative of heat transfer efficiency, can be easily monitored for changes in the control parameters. Since the average Nusselt number of the second source can be written as

$$\mathrm{Nu}_2 = \frac{q_{j,2} \cdot \ell}{\Delta\overline{T}_2 \cdot k_f} \tag{41}$$

where $q_{j,2}$, L and k_f are constant, the mean temperature of the second source can be written as

$$\Delta\overline{T}_2 \propto \frac{1}{\mathrm{Nu}_2} \tag{42}$$

Figure 10 relates the heat dissipated by the various modes of heat transfer, i.e., conduction, convection and radiation, for a range of board thermal conductivities between 0 and 20 $W/m \cdot K$. Three levels of emissivity are presented for each case.

In forced convection, the radiative component of the dissipated heat is generally less than 15% but for most of the range examined the radiative component can be considered constant, in the range of 5%.

When the thermal conductivity of the board is small, the resistance to heat flow under the source is greater than the thermal resistance of the boundary layer and the heat dissipated by convection dominates. However, at a thermal conductivity of approximately 2.5 $W/m \cdot K$ the resistance between the boundary layer and the board are equivalent and the two modes of heat transfer are essentially of equivalent magnitude. For board conductivities greater than 2.5 $W/m \cdot K$ the conduction within the board dominates.

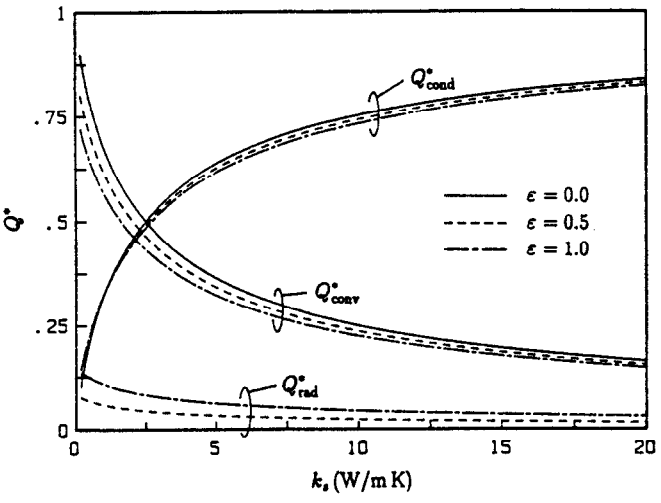

Figure 10: The Relative Contribution of Conduction, Convection and Radiation to Overall Heat Dissipation

The convective fraction decreases with increasing conductivity primarily because the resistance within the board is greater than the resistance in the boundary layer.

Concluding Remarks

Conjugate heat transfer problems of the type described in the previous sections can be extremely complex due to the interaction of the fluid and solid domains and the necessity for the governing equations in each domain to be satisfied simultaneously. Studies of this type are useful for observing the relative importance of basic design parameters in respect to the role they have in controlling local circuit board temperatures. However, for more general studies, in which a variety flow conditions, circuit board geometries and thermophysical properties are studied, a simulation model, such as META, must be used to provide accurate results in a time frame which is conducive to design scheduling.

Acknowledgements

The authors wish to thank the Natural Sciences and Engineering Research Council of Canada for financial support under CRD contract 661-062/88.

References

Culham, J.R. and Yovanovich, M.M., 1987, "Non-Iterative Technique for Computing Temperature Distributions in Flat Plates with Distributed Sources and Convective Cooling", Second ASME–JSME Thermal Engineering Joint Conference, Honolulu, Hawaii, March 22–27.

Culham, J.R., Lemczyk, T.F., Lee, S. and Yovanovich, M.M., 1991, "META - A Conjugate Heat Transfer Model For Cooling of Circuit Boards With Arbitrarily Located Heat Sources," ASME National Heat Transfer Conference, Minneapolis, Minnesota, July 28-31.

Kays, W.M., 1966, *Convective Heat and Mass Transfer*, McGraw-Hill Book Company, Toronto.

Lee, S., Culham, J.R and Yovanovich, M.M., 1991, "The Effect of Common Design Parameters on the Thermal Performance of Microelectronic Equipment: Part I - Natural Convection," ASME National Heat Transfer Conference, Minneapolis, MN, July 28-31.

Lemczyk, T.F., Mack, B.F., Culham, J.R. and Yovanovich, M.M., 1991, "PCB Trace Thermal Analysis and Effective Conductivity," presented at the 7th Annual IEEE Semi Conductor Temperature and Thermal Management Symposium (SEMI-THERM), Phoenix, AZ, February, 1991.